FOUCAULT PENDULUM ON A CHIP: ANGLE MEASURING SILICON MEMS GYROSCOPE

Igor P. Prikhodko, Sergei A. Zotov, Alexander A. Trusov, and Andrei M. Shkel
MicroSystems Laboratory, University of California, Irvine, CA, USA

ABSTRACT

We report detailed characterization of a vacuum sealed angle measuring silicon MEMS gyroscope. The new gyroscope utilizes completely symmetric, dynamically balanced quadruple mass architecture, which provides a unique combination of maximized quality (Q) factors and isotropy of both the resonant frequency and the damping. The vacuum sealed SOI prototype with a 2 kHz operational frequency demonstrated virtually identical X- and Y-mode Q-factors of 1.1 million. Due to the stiffness and damping symmetry, and very low dissipation, the gyroscope can be instrumented for direct angle measurements with fundamentally unlimited rotation range and bandwidth. Experimental characterization of the mode-matched gyroscope operated in whole-angle mode confirmed linear response in excess of ±450 °/s range and 100 Hz bandwidth (limited by the setup), eliminating both bandwidth and range constraints of conventional MEMS rate gyroscopes.

INTRODUCTION

In the past decade micromachined vibratory gyroscopes have received increased attention from automotive and consumer electronics industries. All commercial MEMS gyroscopes are angular rate measuring sensors employing energy transfer from the closed-loop drive to the secondary sense-mode [1]. The resolution and sensitivity of MEMS gyroscopes are often improved by maximizing Q-factors and reducing frequency separation between the two modes [2]. Mode-matched silicon gyroscopes with Q of 100,000 have been demonstrated to provide sub-degree-per-hour bias stability [3]. However, mode matching of a high-Q rate gyroscope typically limits the full-scale range to 10 deg/s and rate bandwidth to 1 Hz. One approach to address these constraints is to design a relatively low-Q gyroscope with sub-micron capacitive gaps required for efficient transduction at a high resonant frequency of 3 MHz [4]. An alternative approach, proposed in this paper, is to operate an ultra high-Q gyroscope in the whole-angle mode (free vibrations), providing direct angle measurements with fundamentally unlimited range and bandwidth.

To enable whole-angle operation, sensor requirements for structural symmetry and Q-factors are more stringent, and call for new design architectures. For instance, the macro-scale hemispherical resonator gyroscope (HRG) with sub-arcsecond angle resolution requires isotropic Q-factors as high as 26 million [5]. Achieving this level of damping and stiffness symmetry across process variations of conventional silicon MEMS technologies is very challenging.

The latest advances in design and packaging of silicon MEMS devices enabled vibratory gyroscopes with Q-factors above 0.5 million [6], inspiring development of angle measuring MEMS gyroscopes. In this paper we report detailed characterization of a vacuum sealed Quadruple Mass Gyroscope (QMG) with isotropic dissipation constant of 3 minutes, which enables angle measurements, Figure 1.

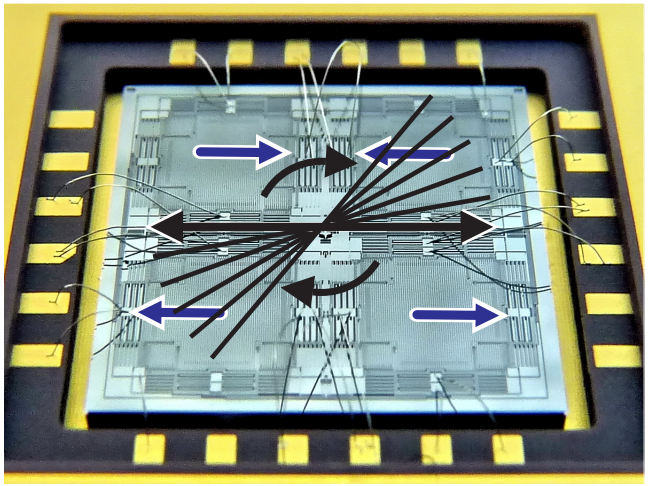

Figure 1: Photograph of a fabricated SOI Quadruple Mass Gyro (QMG) with the illustration of whole-angle operation.

WHOLE-ANGLE MODE OF OPERATION

In this section we describe the operating principle and the fundamental error model for an angle measuring gyroscope.

Whole-Angle Operating Principle

An ideal angle gyroscope is a 2-D isotropic mass-spring system vibrating with the natural frequency ω. In presence of the inertial rotation with the rate Ω, the equations of motion in terms of x, y displacements are:

$$\begin{cases} \ddot{x} + \omega^2 x - 2\Omega\dot{y} = 0, \\ \ddot{y} + \omega^2 y + 2\Omega\dot{x} = 0. \end{cases} \quad (1)$$

The dynamics analysis is simplified when using slow-varying orbital variables a, q, θ, φ, describing semi-major, semi-minor axes, the precession angle, and the orbital phase of the elliptical trajectory, respectively [7]. System (1) becomes:

$$\dot{a} = 0, \quad \dot{q} = 0, \quad \dot{\theta} = -\Omega, \quad \dot{\varphi} = \omega. \quad (2)$$

From the instrumentation point of view, a and q are the amplitude components in-phase and in-quadrature with the reference phase φ. The precession angle θ provides a direct instantaneous measure of the gyroscope rotation:

$$\theta = -\int \Omega dt. \quad (3)$$

This equation describes the governing principle for the whole-angle operation, Figure 2. The whole-angle mode is based upon the classical Foucault pendulum operation, where the axis of vibration is allowed to precess freely in

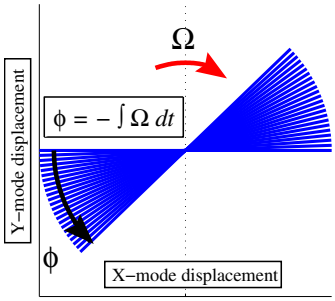

Figure 2: Whole-angle mode: the orientation reference remains fixed in the inertial space, enabling angle detection.

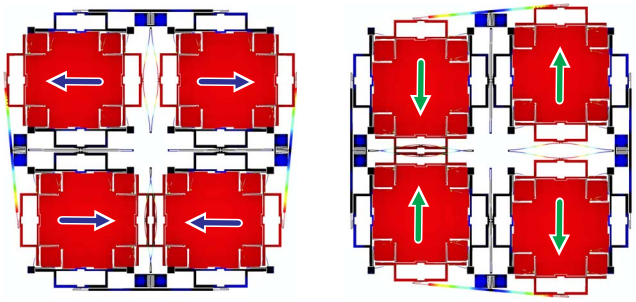

Figure 3: Degenerate, anti-phase X- and Y-vibratory modes of dynamically balanced Quad Mass Gyroscope, modeling.

response to the inertial rotation. Orientation of the free vibrating axis remains fixed in the inertial space, thereby providing an instantaneous orientation reference. Unlike the conventional rate measuring mode, where the axis of vibration is locked to the intended drive direction, the whole-angle mode is not limited in rate range or bandwidth [7].

Changes in the precession angle θ are detected by monitoring x and y displacement components according to:

$$\theta = \text{atan}(||y||/||x||) \quad (4)$$

This simple relation is used to determine the instantaneous angle of rotation from the vibration amplitudes $||x||$, $||y||$.

Whole-Angle Gyroscope Error Model

The above conceptual analysis of the whole-angle operating mode assumes isotropic stiffness and negligible damping. The angle drift in presence of imperfections was derived in [7] by the method of averaging. For mismatches $\Delta\omega = (\omega_1^2 - \omega_2^2)/2\omega$ in frequencies ω_1, ω_2, and $\Delta(1/\tau) = 1/\tau_1 - 1/\tau_2$ energy dissipation time constants τ_1, τ_2, the drift is:

$$\dot{\theta} = \frac{1}{2}\Delta\left(\frac{1}{\tau}\right)\sin 2(\theta - \theta_\tau) + \Delta\omega\cos 2(\theta - \theta_\omega)\frac{aq}{a^2 - q^2} - \Omega, \quad (5)$$

where θ_τ, θ_ω are the angles of the τ_1 and ω_2 principal axes of damping and elasticity, respectively. The orbital parameters a, q are no longer constants, but time-varying variables.

Equation (5) reveals the periodic nature of the angle drift; errors are averaged out for fast spinning objects. The minimum detectable angle derived from (5) is limited by the mismatches in device damping and frequency:

$$\left|\dot{\theta}_{drift}\right| \le \left|\Delta(1/\tau)\right|/2 + (q/a)\left|\Delta\omega\right|. \quad (6)$$

In practice, the term $(q/a)|\Delta\omega|$ is compensated either by electrostatic or mechanical trimming of stiffness asymmetry to null $\Delta\omega = 0$, or by quadrature control to null $q = 0$ [8].

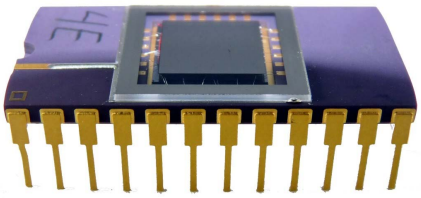

Figure 4: Photograph of a stand-alone vacuum packaged QMG prototype lid sealed at 0.1 mTorr with getter material.

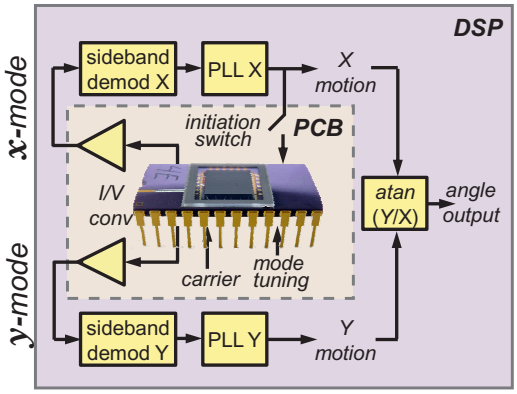

Figure 5: Instrumentation of a whole-angle gyroscope.

In contrast, the damping asymmetry is the major drift source in angle measuring MEMS, and requires highly isotropic Q-factors to overcome this problem. For instance, the damping asymmetry $\Delta(1/\tau)$ of 10^{-5} s^{-1} with τ of 160 s (equivalently, $\Delta Q/Q$ of 0.1%) leads to the drift of 1 °/hour, and can be reduced by maximizing Q. These considerations motivate the development of an inherently symmetric gyroscope structure with ultra-high Q-factors.

SENSOR DESIGN AND INSTRUMENTATION

In this section we report the sensor design, fabrication and interface electronics used in the experimental study.

Sensor Design Concept

In comparison to the precision machined, axisymmetric HRG, previously investigated silicon MEMS gyroscopes suffered from aniso-elasticity, aniso-damping, and short energy dissipation constant less than 1 second. The novel z-axis MEMS angle measuring sensor utilizes a completely symmetric quadruple mass architecture [6], which provides an advantageous combination of low energy dissipation and isotropy of both the resonant frequency and the damping.

The structure is comprised of four symmetrically decoupled tines synchronized by anti-phase levers, which provide vibration isolation and suppress temperature drifts, Figure 3. Due to symmetry, X- and Y-modes are degenerate and are spatially oriented at a 90° angle. This design enables whole-angle mode based on free vibrations of the inertial mass, with the precession angle equal to the rotation angle.

Prototype Fabrication and Vacuum Packaging

The QMG prototypes were fabricated using an in-house, wafer-level, single-mask process based on silicon-on-insulator (SOI) substrates with 100 μm thick device layer

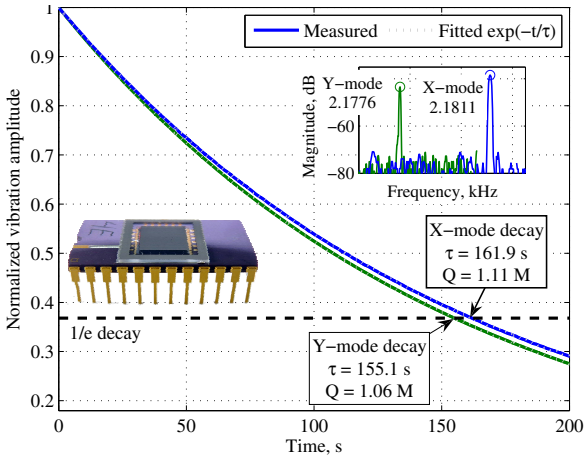

Figure 6: Structural characterization of the vacuum sealed QMG using ring-down tests. X-mode Q-factor of 1.11 and Y-mode Q of 1.06 million approach the fundamental thermoelastic limit of 1.3 million. Inset: power spectrum.

and a 5 µm buried oxide layer. Sensors were defined in a highly doped (boron concentrations of 10^{20} cm^{-3}) device layer by DRIE. Stand-alone ultra-high Q sensors, Figure 4, were obtained by using a package-level technology [9] for robust vacuum sealing. First, the gyroscope die was attached to ceramic package using eutectic solder, and then wire bonded. The device was sealed at sub-mTorr vacuum, preceded by a getter activation on a glass lid.

Interface Electronics

Devices were tested using PCB electronics connected to the digital signal processing unit. The sensors were mounted on a PCB with front-end transimpedance amplifiers. All signal processing was performed in real-time using a FPGA-based lock-in amplifier from Zurich Instruments, Figure 5.

EXPERIMENTAL CHARACTERIZATION

In this section we experimentally evaluate structural symmetry and whole-angle operation of a QMG prototype. All experiments presented here were performed using a vacuum sealed QMG operating in free vibrations. To initiate vibrations, the gyroscope with 2 kHz operational frequency was electrostatically driven into the X-mode anti-phase resonant motion, Figure 3, using a phase-locked loop, which was then abruptly turned off. An Electromechanical Amplitude Modulation technique was used to detect the motion of X- and Y-modes (amplitude and phase), Figure 5.

Structural Characterization

The dynamically balanced, geometrically symmetric design of the QMG is expected to provide identical Q-factors. The damping symmetry of a stand-alone QMG prototype was investigated using ring-down tests. The time-domain amplitude decays of X- and Y-modes were fitted with exponential decays to extract time constants τ of 162 s and 155 s, respectively, Figure 6. The Q-factors were calculated according to $Q = \pi f_n \tau$ with natural frequencies f_n of approximately 2.2 kHz provided by PLLs. Measured X-

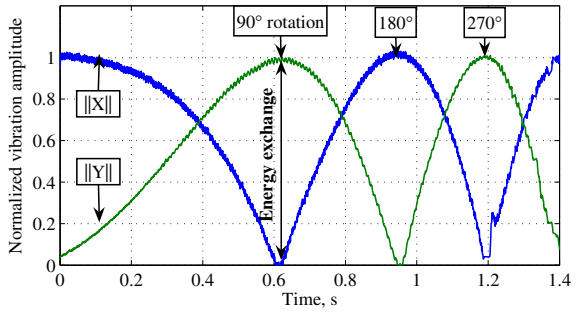

a) Measured vibration amplitudes of X- and Y- modes in response to the rotation with 280 °/s² acceleration.

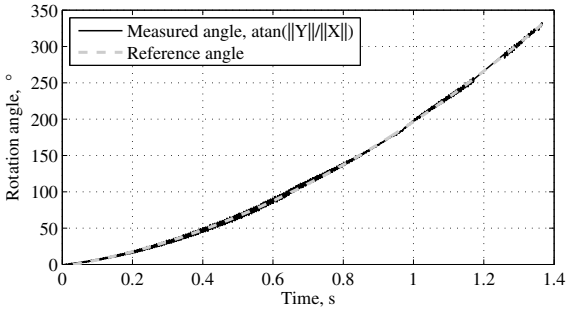

b) Direct angle measurement derived from atan(||Y||/||X||).

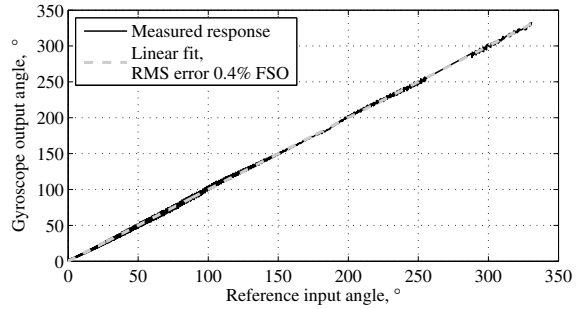

c) Measured angle response demonstrates sensor linearity.

Figure 7: Whole-angle mode characterization using QMG.

mode Q of 1.11 and Y-mode Q of 1.06 million approach the fundamental thermoelastic limit of 1.3 million. Structural characterization revealed virtually identical X- and Y-mode time constants of 160 s, providing ~10 minutes operating time in the free vibrations regime. The data confirms the design hypothesis of the inherent Q-factor symmetry in QMG structures.

Whole-Angle Mode Characterization

Both the damping symmetry and the ultra-high Q-factors are expected to allow whole-angle measurements. Angle response characterization was performed using the stand-alone QMG prototype operating in free vibrations. First, the 20 mHz frequency mismatch between the X- and Y-modes was achieved by the electrostatic tuning. The device was then rotated with a constant angular acceleration of 280 °/s², providing input rates of 0 to 450 °/s, Figure 7.

The instantaneous position of the axis of vibration was detected capacitively by monitoring the displacement of X- and Y-modes. The amplitude change of X- and Y-modes was recorded in response to a rotation with a 280 °/s²

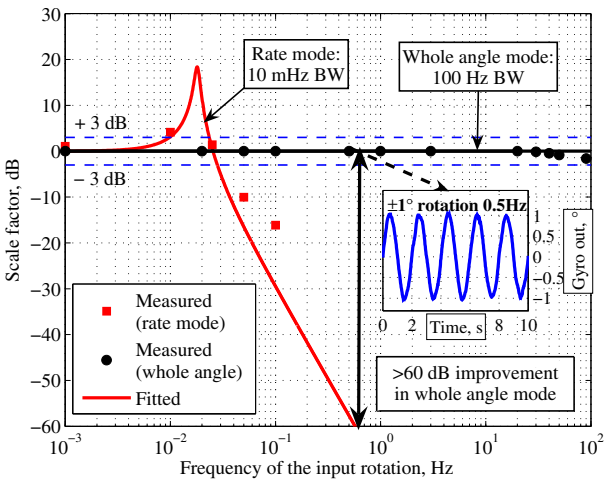

Figure 8: Experimental comparison of the QMG gyroscope bandwidth, demonstrating 60 dB improvement when operated whole-angle mode in comparison to the rate mode.

angular acceleration, Figure 7(a). Initially, the device was vibrating in X-direction, and after a 90 ° rotation the proof-mass was oscillating in the Y-direction. The subsequent 90 ° rotation causes the device to vibrate again in the X-mode. These energy transfers between the X- and Y-modes serve as the basis for the angle detection. The precession angle of the vibration pattern was computed in real time from the amplitudes of X- and Y-modes using the simple relation $\theta = \text{atan}(||Y||/||X||)$, Figure 7(b). The measured angle response confirmed orientation-independent angular gain, and sensor linearity with 0.4% RMS error FSO, and Figure 7(c).

The input dynamic range of the whole-angle mode is fundamentally unlimited due to the free, unconstrained precession of the axis of vibration in response to the device rotation. Characterization of the whole-angle mode revealed wide dynamic range in excess of 450 °/s (limited by the experimental setup), thereby combining advantages of both maximized *Q*-factors and precision of the mode-matched gyroscopes.

Bandwidth Analysis

The whole-angle operating mode is also expected to provide unlimited measurement bandwidth. The bandwidth of mode-matched ultra-low dissipation QMG device was characterized for both conventional rate measuring (forced vibrations) and whole-angle modes (free vibrations). Scale factors were measured for periodic rotations with the frequencies up to 100 Hz (limited by the setup). Scale factors of the rate operating mode were normalized to the constant rotation and compared to the angular gain factors of the whole-angle mode, Figure 8. Characterization of the whole-angle operating mode revealed a bandwidth in excess of 100 Hz, which is a 10,000 improvement over the conventional rate mode with a 10 mHz bandwidth.

CONCLUSIONS

We demonstrated the silicon MEMS angle measuring gyroscope enabled by the geometrically symmetric QMG design and unprecedented ultra-high *Q*-factors. The vacuum sealed SOI prototype with a 2 kHz operational frequency demonstrated virtually identical X- and Y-mode *Q*-factors of 1.1 million, approaching the thermoelastic limit of 1.3 million. This allows for a power failure-independent operation with polarization voltages as low as 10 mV dc previously achieved only in HRG for space-flight missions [5]. Due to stiffness and damping symmetry, and ultra-low dissipation, this gyroscope was instrumented for the direct measurements of the angle with fundamentally unlimited input range and bandwidth. Experimental characterization of the mode-matched gyroscope operating in the whole-angle mode confirmed linearity in excess of ±450 °/s range and 100 Hz bandwidth, eliminating both bandwidth and range constraints of conventional MEMS rate gyroscopes.

ACKNOWLEDGMENTS

This work was funded by ONR/NSWCDD grant No. N00014-09-1-0424. Authors would like to thank Dr. Flavio Heer from Zurich Instruments AG for assistance with signal processing; Heather Florence of SAES Getters and Paul Barnes of SST International for assistance with vacuum packaging. The gyroscopes were designed, fabricated, and characterized at the UC Irvine MicroSystems Laboratory.

REFERENCES

[1] A.M. Shkel, "Type I and Type II Micromachined Vibratory Gyroscopes," *Proc. IEEE/ION PLANS 2006*, pp. 586–593, 2006.

[2] M. Weinberg et al., "Energy Loss in MEMS Resonators and the Impact on Inertial and RF Devices," *Proc. Transducers 2009*, pp. 688-695, 2009.

[3] M.F. Zaman, A. Sharma, Z. Hao, F. Ayazi, "A Mode-Matched Silicon Yaw Tuning-Fork Gyroscope with Subdegree-per-hour Allan Deviation Bias Instability," *IEEE JMEMS,* vol.17, no.6, pp.1526-1536, 2008.

[4] W.K. Sung, M. Dalal, F. Ayazi, "A 3MHz spoke gyroscope with wide bandwidth and large dynamic range," *Proc. IEEE MEMS 2010*, pp. 104-107, 2010.

[5] D.M. Rozelle, "The Hemispherical Resonator Gyro: From Wineglass to the Planets," *Proc. 19th AAS/AIAA Space Flight Mechanics Meeting 2009*, pp. 1157-1178.

[6] A.A. Trusov, I.P. Prikhodko, S.A. Zotov, A.R. Schofield, A.M. Shkel, "Ultra-High Q Silicon Gyroscopes with Interchangeable Rate and Whole Angle Modes of Operation," *Proc. IEEE Sensors 2010*, pp. 864-867, 2010.

[7] D.D. Lynch, "Vibratory Gyro Analysis by the Method of Averaging," *Proc. 2nd St. Petersburg Conf. on Gyroscopic Technology and Navigation*, 1995.

[8] C.C. Painter, A.M. Shkel, "Active Structural Error Suppression in MEMS Vibratory Gyroscopes," *Proc. IEEE Sensors 2002*, pp. 1089-1094, 2002.

[9] A.R. Schofield, A.A. Trusov, A.M. Shkel, "Versatile Sub-mTorr Vacuum Packaging for the Experimental Study of Resonant MEMS," *Proc. IEEE MEMS 2010*, pp. 516-519, 2010.